



**HAL**  
open science

# A Novel Robot Soft Cover with Thermal Display Capabilities

Yukiko Osawa, Abderrahmane Kheddar

► **To cite this version:**

Yukiko Osawa, Abderrahmane Kheddar. A Novel Robot Soft Cover with Thermal Display Capabilities. 2020. hal-02491308v1

**HAL Id: hal-02491308**

**<https://hal.science/hal-02491308v1>**

Preprint submitted on 25 Feb 2020 (v1), last revised 14 Oct 2021 (v2)

**HAL** is a multi-disciplinary open access archive for the deposit and dissemination of scientific research documents, whether they are published or not. The documents may come from teaching and research institutions in France or abroad, or from public or private research centers.

L'archive ouverte pluridisciplinaire **HAL**, est destinée au dépôt et à la diffusion de documents scientifiques de niveau recherche, publiés ou non, émanant des établissements d'enseignement et de recherche français ou étrangers, des laboratoires publics ou privés.

# A Novel Robot Soft Cover with Thermal Display Capabilities

Yukiko Osawa<sup>1</sup> and Abderrahmane Kheddar<sup>2</sup>

**Abstract**—There is a considerable amount of studies focusing on ‘intelligence’ in planning and control to implement effective human-robot physical interaction. However, physical interaction between humans and robots also pertains ‘intelligence’ in terms of hardware, and more particularly the interfacing cover, often called artificial skins. How to design covers that gathers both functionalities (e.g. softness, sensing) and aesthetic (e.g. pleasant to human sight and touch) is a very challenging problem. In this letter, we propose a prototype of a robot cover that achieves thermal display while being also soft. This is because previous human studies have identified thermal cues as part of the touch pleasantness feeling. In order to realize both softness and high thermal conductivity, the developed cover embed an urethane pipe within which water flows. The soft cover becomes hot or cold by controlling the temperature of the flowing water. The algorithm for regulating the cover’s temperature for display is similar to the human blood system, which is simple but effective. We assess our developed cover with some experiments.

## I. INTRODUCTION

Efficient physical human-robot interaction (pHRI for short) enables several new robotic domains of applications. The most known examples are cobotics in industry and motion assistance through contact for frail persons. The robot can benefit from contact in interactive pHRI to achieve various tasks with the human. Yet, pHRI requires high safety considerations and sophisticated planning and control strategies, but not only. Indeed, current pHRI studies are mainly focusing on the planning, the control with human in the loop, and functional cover (robot skins). We claim that the interaction between humans and robots must also be considered from an aesthetic and pleasantness (to human touch) hardware design viewpoint. In our view, combining functionalities to aesthetic and pleasantness is a new important challenge to investigate. Yet, softness is very likely at the intersection of both functionality (casting the environment irregularities, absorbing impacts, safety through inherent compliance, etc.) and pleasantness to touch when compared to a rigid cover.

Pleasant touch could be important for human motion assist applications, but also for programming by demonstration in cobotics. For example, a gentle stroking touch lower blood pressure, increase transient sympathetic reflexes [1] and increase pain thresholds [2]. There are some studies for analyzing touch pleasantness. Force of a finger sliding

\*This work was supported by JSPS Overseas Research Fellowships No.201960463 and the CNRS-Mitsui Chemical joint research agreement.

<sup>1</sup>CNRS-University of Montpellier, LIRMM, Interactive Digital Humans group, Montpellier, France yukiko.akiyama@lirimm.fr

<sup>2</sup>CNRS-University of Montpellier, LIRMM, Interactive Digital Humans group, Montpellier, France kheddar@lirimm.fr

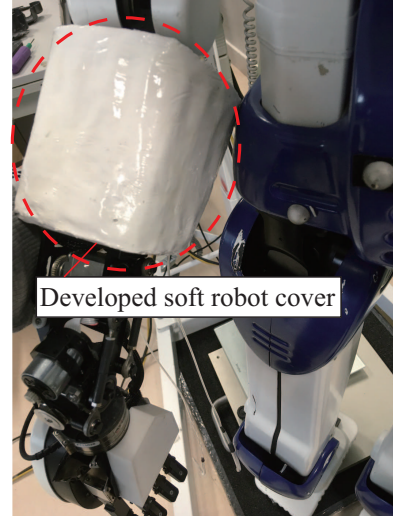


Fig. 1. Novel soft-thermal display robot cover developed in this letter and mounted on the humanoid HRP-4 forearm.

was analyzed in the spatial domain, and it follows  $1/f$  noise that is related to relaxation oscillation [3]. From [4], it was found that frictional force fluctuations are correlated with the pleasantness sensation of surfaces using the Pleasant Touch Scale determined by fingertip moisture level and sensory evaluation. In particular, the human thermal sensation is related to pleasantness. The tactile C afferent in which the firing rate is correlated with hedonic ratings discharged typical skin temperature (about  $32^{\circ}\text{C}$ ) rather than the cooler and warmer stimulus temperatures [5]. According to [6], dynamic thermal stimuli are less pleasant than constant thermal stimuli, and  $4^{\circ}\text{C}$  increase from the skin temperature was rated as arousing, dominant, and pleasant. The studies in [7], [8] show that warmth in physical interactions with mediated touch devices gives us beneficial effects. Therefore, covering the robot by a thermally conductive material is one of the essential features for providing a pleasant feeling. Moreover, actively changing warmness could be viewed as part of haptic communication in pHRI.

### A. Related work

The research topic about soft material covering a robot –often called robot skin, has been studied since many years. To create a robot skin that is light and soft, some studies exploited the air pressure feedback controller. Soft skin module with a built-in airtight cavity in which air pressure can be sensed was developed in [9]. Authors in [10] proposed soft robotic gripper with silicone elastomer and pneumatic

chambers, and stretchable elastomer skin that can be actively inflated and deflated is also developed [11]. Besides, the study [12] developed stretchable electroluminescent using a pneumatic chamber. The silicone structure for the 3-axis force measurements was proposed [13], and the literature [14] installed the flexible skin for sensing force to the robot arm and tested in pHRI applications. As for the control scheme for soft robot skin, the study [15] mentioned how to create a feedforward model by learning model parameters. The controller for generating virtual compliant forces of the robot skin was also proposed [16]. In a different approach, artificial skins for attaching to robots have been researched. The study [17] proposed the soft artificial skin that has a multilayered sensor circuit for detecting multi-axis strains and contact pressure. The stretchable capacitive sensory skin was also developed in [18]. In addition, the artificial skin for a humanoid robot using a mesh of triangular sensor modules was proposed [19].

As for thermal cues, there are many studies for reproducing thermal sensations in the telepresence haptics research fields. Most studies use a thermo-electronic module (TEM) –called Peltier pump, as a thermal actuator. The device can generate a temperature difference between the front and backside of the device, thanks to the Peltier effect. The studies [20], [21] developed dynamic thermal displays using Peltier pumps as haptic devices. There are a lot of control strategies of the device for rendering thermal sensations, such as methods of temperature control [22], [23], and heat flow control [24]. Authors in [25] also proposed the wearable thermal display using nichrome wire. The literatures [26], [27] were the first to propose thermal bilateral controllers for Peltier pump by considering both temperature and heat flow bilateral coupling. Besides, the study [28] extended the rendering area by using heat conduction from the Peltier pump.

Achieving both soft and thermal rendering in one robot cover was not yet achieved to our best knowledge. There are some problems with covering robot with a material that combine both softness and thermal conductivity;

- Most soft material with relatively low mass density such as silicone and rubbers have relatively low thermal conductivity;
- Soft cover would be hardened when they embedded (within the material or on its surface) with heat sources, sensors, or heat conduction materials.

To tackle these limitations, we developed a novel robot cover that combines softness with thermal rendering.

### B. Our contribution

In this letter, we propose a novel design of a robot soft cover and its control system for rendering desired thermal response (cooling or heating) at will. The Fig. 1 shows the developed robot cover mounted in the HRP-4 forearm. It includes an urethane pipe in which water circulates according to a desired flow. The cover becomes hot or cold depending on water temperature, which is controlled in closed-loop. The algorithm for the heating and cooling system is similar

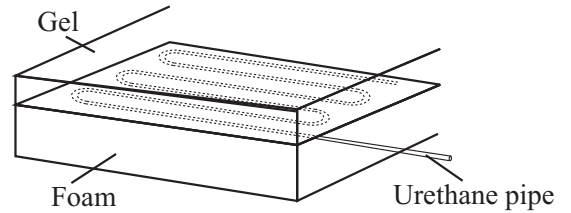


Fig. 2. Structure of the soft robot cover.

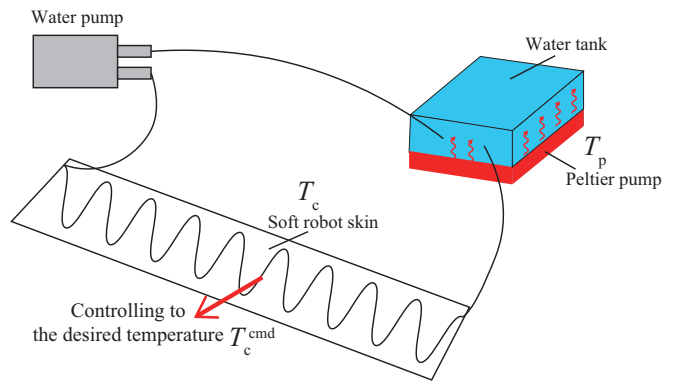


Fig. 3. Overall system for controlling the soft robot cover (the water system).

to the human blood system or car engine cooling principle: it is simple and effective. Two kinds of materials consisting of the cover that has high heat conductivity and low density made it possible to be soft, well thermally conductive, and light. There is a general problem of robot skin that the heat generated from the robot’s embedded actuators will not dissipate appropriately by covering the robot. Moreover, most of the soft material has low heat conductivity and covering the robot by soft material is generally difficult. We solved this problem by using flowing water with the Peltier pump that can both heat and cool it. Experiments were conducted to assess the developed soft thermal robot cover.

### C. Paper organization

This letter is organized as follows. Section II presents a structure of the developed robot cover. The model of the water system, including the Peltier pump, is explained in Section III. Section IV states the control system for giving a desired thermal response of the cover. Section V shows the experimental results for assessing the robot cover. This letter is concluded in Section VI.

## II. STRUCTURE OF THE DEVELOPED ROBOT COVER

### A. Thermal properties of the robot cover

Figure 1 shows our designed composite soft and thermal robot cover. The prototype is made to cover the forearm of the humanoid robot HRP-4. Hence, it has an areas of  $11.0 \times 31.0 \text{ cm}^2$  to be put around the right arm. The reason for this choice is to investigate in the future a humanoid robot supporting frail humans motion for daily assistance. One can imagine the robot as a reconfigurable hurdle and the human would put one of her/his hands on the robot arm to help for example in a site-to-stand motion, see illustrations in [29]. The soft cover is structured into two layered materials as shown in Fig. 2. In between the two materials, we embedded (prior to gluing to two) an urethane pipe having 2 mm of outer diameter. A controlled temperature water would then flow through this urethane pipe. The upper (gel) part would conduct and hence diffuse the temperature. The foam part, being not thermally conductive, would simply isolate the inner robot body. Moreover, the chosen foam material has a very low mass density and good compliance properties, which allows designing an overall light whole-body cover that is soft with thermal rendering capabilities.

The gel that we used was customized from Mitsui Chemicals, and it has higher heat conductivity ( $0.37 \text{ W/mK}$  at  $23^\circ\text{C}$ ) with respect to know existing gels. Therefore, it is able to transfer temperature from the water flowing inside of the pipes (the urethane pipe has heat conductivity  $0.025 \text{ W/mK}$  [30] being also conductive, but clearly less than the gel). The gel layer is made thin because the gel has high mass density and hence is heavier than the foam. The thickness of the gel and foam layer is 2 mm and 5 mm, respectively. The overall cover thickness is thus 7 mm. Ideally we would choose the thickness to meet desired compliance of the cover while being the thinner possible. Indeed, by having thin covers we do not increase substantially the mass of the robot and keep a good range of motion of each link, as otherwise we would jeopardize the range of the articulations, see a method for computing the thickness in [31]. At this end, our proposed cover achieves two antagonistic properties: softness and high thermal conductivity at the same time. The water will end in a accumulator tank where it will be heated or cooled using the Peltier effect [32].

### B. Overall system

The overall system is illustrated in Fig. 3. It consists of a small water pump; a copper tank –on top of which is mounted a Peltier pump acting as a heat source; and finally, the soft robot cover explained previously. The water pump, the tank, and the robot cover are connected by the pipe of which diameter is 4.5 mm. The water stored in the tank is heated and cooled by the Peltier pump. It is flowed thanks to the water pump, which can regulate the flow of the water to circulate in a closed-circuit throughout our proposed cover. Thermocouples, measuring temperature, are attached to the surface of the heat source and others to the soft robot cover. In this latter, we refer to this system as “the water

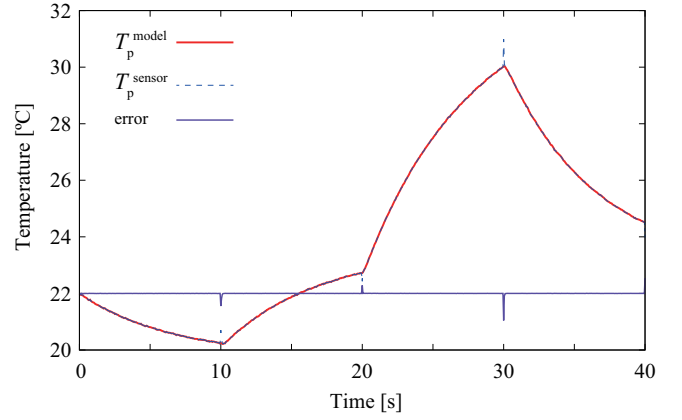


Fig. 4. Assessment for Peltier pump model.

system”. The effect of the water system is confirmed by the experimental results shown in Sec. V.

## III. MODELING OF THE WATER SYSTEM

This section is dedicated to modeling of the main components of the water system, in order to be controlled.

### A. Modeling the Peltier pump with ARMA model

The temperature of the robot cover is controlled mainly by the Peltier pump attached to the water tank. In order to account for the nonlinear behavior of the Peltier pump, a discrete-time autoregressive moving average (ARMA) model is used [33] for temperature controlling. The dynamic behavior of the Peltier pump temperature  $T_p$  is derived as

$$T_p(t) = - \underbrace{\sum_{i=1}^n \sum_{k=0}^p a_{ik} I(t-i)^k T(t-i)}_{\text{AR part}} + \underbrace{\sum_{j=1}^m \sum_{h=0}^q b_{jh} I(t-j)^h I(t-j)}_{\text{MA part}}. \quad (1)$$

The underlined parts of (1) are parameters depending on the current  $I(t)$ , where  $a_{ik}$ ,  $b_{jh}$ ,  $p$ , and  $q$  are constant parameters and the number of  $k$  and  $h$ , respectively. The parameters  $i$  and  $j$  denote discrete time of  $I(t)$  and  $T(t)$ , and  $n$ ,  $m$  represent the order of the ARMA model, respectively. The model can be classified as unknown parameters  $\theta$  and known parameters  $\varphi(t)$ , expressed as

$$T_p(t) = \theta^T \varphi(t) \quad (2)$$

$$\theta = [a_{ik}\{i = 1 \dots n, k = 0 \dots p\}; b_{jh}\{j = 1 \dots m, h = 0 \dots q\}] \quad (3)$$

$$\varphi(t) = [I(t-i)^k T(t-i)\{i = 1 \dots n, k = 0 \dots p\}; I(t-j)^{h+1}\{j = 1 \dots m, h = 0 \dots q\}]. \quad (4)$$

In this letter, the order of the model  $n$ ,  $m$ ,  $p$ ,  $q$  is set to 3 which proved to be a good compromise between accuracy and complexity of the model. Higher orders do not improve substantially (i.e. w.r.t the measurements precision)

TABLE I  
IDENTIFICATION RESULTS OF THE PELTIER PUMP.

Parameter	Value
$a_{10}$	-0.3367
$a_{11}$	-0.1499
$a_{12}$	-0.6423
$a_{20}$	-0.3334
$a_{21}$	-0.1528
$a_{22}$	-0.6076
$a_{30}$	-0.3298
$a_{31}$	-0.1637
$a_{32}$	-0.5643
$b_{10}$	-0.3714
$b_{11}$	0.2779
$b_{12}$	-0.4374
$b_{20}$	-0.3537
$b_{21}$	0.2727
$b_{22}$	-0.2969
$b_{30}$	-0.3206
$b_{31}$	0.2613
$b_{32}$	-0.0103

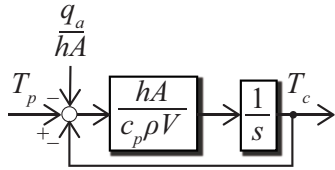


Fig. 5. Block diagram of the water system.

the performances. The unknown parameters are estimated using the recursive least square method (RLSM) derived as

$$\hat{\theta}(t) = \hat{\theta}(t-1) + \frac{K(t-1)\varphi(t)(T_p(t) - \hat{\theta}^T(t-1)\varphi(t))}{\lambda + \varphi(t)^T K(t-1)\varphi(t)}, \quad (5)$$

where  $\hat{\theta}(t)$ ,  $\lambda$  and  $K(t)$  stand for the estimated value at  $t$ , the forgetting factor, and the Kalman matrix gain, respectively. The Kalman gain is updated as

$$K(t) = \frac{1}{\lambda} \left( K(t-1) - \frac{K(t-1)\varphi(t)\varphi^T(t)K(t-1)}{\lambda + \varphi(t)^T K(t-1)\varphi(t)} \right). \quad (6)$$

Figure 4 shows measured temperature of the Peltier pump comparing with the estimated value and its errors. In this experiments, the initial Kalman matrix gain  $P_0$  is set to 1000, and the forgetting factor  $\lambda$  is set to 0.995, which means that the memory horizon ( $\gamma = \frac{1}{1-\lambda}$ ) is 200. These values were decided based on [34]. The current inputs applied to the Peltier pump were as follows:

- 0 s-10 s: Current input...0.6 A
- 10 s-20 s: Current input...0.3 A
- 20 s-30 s: Current input...-0.5 A
- 30 s-40 s: Current input...0.4 A

From this figure, the estimated temperature follows the measured temperature, except the moment rapidly changing of the current input. The identification results of the Peltier pump from the RLSM is shown in Table I.

TABLE II  
PARAMETERS OF THE WATER SYSTEM.

Parameter	Description
$t$	Time [s]
$t_s$	Sampling time [s]
$T$	Temperature [ $^{\circ}$ C]
$T_p$	Temperature of the Peltier pump [ $^{\circ}$ C]
$T_c$	Temperature of the robot cover [ $^{\circ}$ C]
$I$	Current [A]
$c_p$	Specific heat of water [kJ·K/kg]
$h$	Convection heat-transfer coefficient [W/m <sup>2</sup> K]
$k_c$	Thermal conductivity [W/mK]
$v$	Velocity of water flow [m/s]
$\rho$	Density [kg/m <sup>3</sup> ]
$d$	Diameter of the pipe [m]
$L$	Length [m]
$A$	Area [m <sup>2</sup> ]
$V$	Volume [m <sup>3</sup> ]
$\mu$	Viscosity [kg/ms]
$q_a$	Heat loss [W]
$R$	Thermal resistance [K/W]
Nu	Nusselt number
Re	Reynolds number
Pr	Prandtl number
Subscript $d$	Representative length
Subscript $p$	Peltier pump
Subscript $c$	Robot cover
Subscript $a$	Ambient temperature
○	Average value
⊙	Estimated value

## B. Modeling of the water system

1) *Heat convection from the Peltier pump:* Parameters using for the model of the water system are summarized in Table II. The variation of internal energy of the water system is equal to the heat transfer from the Peltier pump to the surface of the cover shown as

$$c_p \rho V \frac{dT_c}{dt} = hA(T_p - T_c) - q_a \quad (7)$$

$$q_a = \frac{(T_c - T_a)}{R_a}, \quad (8)$$

where  $T_c$ ,  $T_p$ ,  $T_a$ ,  $c_p$ ,  $\rho$ ,  $h$ ,  $V$ , and  $A$  are temperature of the cover, the Peltier pump, ambient temperature, specific heat and density of water, convection heat-transfer coefficient, volume and area of water tank, respectively. Here,  $q_a$  is defined as a heat loss from the surface of the cover to the air. By the Laplace transformation based on (7), the heat convection from  $T_p$  to  $T_c$  can be computed as

$$T_c = \frac{\frac{hA}{c_p \rho V}}{s + \frac{hA}{c_p \rho V}} \left( T_p - \frac{q_a}{hA} \right), \quad (9)$$

where  $s$  is the Laplace operator. From (9), the water system can be expressed as first-order system, and its block diagram is shown in Fig. 5.

2) *Velocity of water flow and heat-transfer coefficient:* The heat-transfer coefficient  $h$ , being included in (9), changes depending on the velocity of the water flow. The parameter  $h$  is expressed using the Local Nusselt number Nu as

$$h = \frac{k_c}{d} \text{Nu}, \quad (10)$$

TABLE III  
PARAMETERS FOR THE SIMULATION.

Parameter	Description	Value
$t_s$	sampling time	1.0 ms
$k_c$	Thermal conductivity	0.125 m W/mK
$c_p$	Specific heat of water	4.208 kJ-K/kg
$\rho$	Density	999.8 kg/m <sup>3</sup>
$\mu$	Viscosity	1.55 kg/ms
$R_a$	Thermal resistance of air	3200 K/W
$d$	Diameter of the pipe	$4.5 \times 10^{-3}$ m
$L$	Length	2.3 m
$A$	Area	$3.2 \times 10^{-3}$ m <sup>2</sup>
$V$	Volume	$3.2 \times 10^{-5}$ m <sup>3</sup>
Pr	Prandtl number	11.35

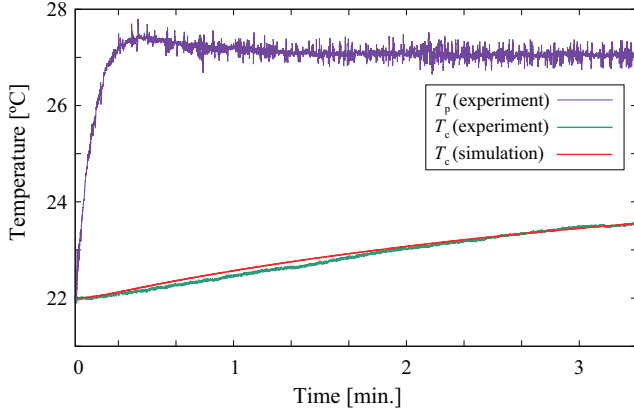


Fig. 6. Verification for the model of the water system.

where  $k_c$  and  $d$  stand for thermal conductivity and diameter of water flow, respectively. As for Nu, there are two types of models; turbulent flow and laminar flow that are classified by the Reynolds Number (Re). The Reynolds number Re is calculated as

$$\text{Re} = \frac{vd\rho}{\mu}, \quad (11)$$

where  $v$  and  $\mu$  are velocity and viscosity, respectively. Considering the maximum velocity of the water pump used in this letter, the value of Re is less than 2300 and the model of laminar flow was used for heat-convection model. The empirical relationship for laminar flow [30], [35] has been used for calculating average Nusselt number shown as

$$\overline{\text{Nu}}_d = 3.66 + \frac{0.0668 (d/L) \text{Re}_d \text{Pr}}{1 + 0.04 ((d/L) \text{Re}_d \text{Pr})^{2/3}}, \quad (12)$$

where subscript  $d$ ,  $L$ , and Pr are diameter of the pipe, length of the pipe and the tank, and Prandtl number, respectively. Using (10), (11) and (12), heat transfer coefficient can be expressed as

$$h = \frac{k_c}{d} \left( 3.66 + \frac{0.0668 (d/L) \left( \frac{\rho v d}{\mu} \right) \text{Pr}}{1 + 0.04 \left( (d/L) \left( \frac{\rho v d}{\mu} \right) \text{Pr} \right)^{2/3}} \right). \quad (13)$$

The equation (13) shows that  $h$  changes depending on the velocity of water flow  $v$ .

3) *Model identification*: Figure 6 shows simulation results of temperature dynamics of the cover derived from (9) and (13) compared to the experimental results. The parameters for this simulation are shown in Table III, using from the theoretical values of water properties (37.78°C) [30]. The command value for the velocity of the water pump keeps 3.22 m/s, and Re becomes 9.36 which means the water flow is laminar flow that can be expressed as (12). The value of thermal conductivity of the water system  $k_c$  was determined by identification. This value was quite low comparing to the theoretical one because of heat loss through the pipe. The simulation was conducted using the experimental temperature response of the Peltier pump. In Fig. 6, we illustrate that the model derived from the theoretical equations matches that of the real experimental system.

#### IV. CONTROL STRUCTURE OF THE WATER SYSTEM

The water system has two controllable inputs: (i) the temperature of the Peltier pump attached to the water tank, and (ii) the water flow velocity that can be changed by the voltage command of the water pump. The system can be described as

$$u_1 = T_p \quad (14)$$

$$u_2 = v \quad (15)$$

$$\dot{T}_c = -\frac{h(u_2)A}{c_p\rho V}T_c + \frac{h(u_2)A}{c_p\rho V}(u_1 - q_a), \quad (16)$$

where  $u_1$  and  $u_2$  are inputs of this system. As mentioned in (13) at Sec. III-B.2, the velocity of the water flow is related to the convection heat-transfer coefficient  $h$ . Here, the velocity of the water flow can not be measured directly, and the velocity command of the water pump was regarded as  $v$  in the control system. To linearize the model of the water system, a constant voltage command is applied to the water pump in this letter. In the control system, a model preview controller (MPC) is used to regulate the temperature of the robot cover because of two reasons: (i) the control system will be extended to two inputs system in future work, because we might need to develop a local regulator for the flow, and (ii) the system includes some constraints. By considering  $u_2$  as constant, the continuous model shown in (16) is converted to the discrete model as:

$$T_c(k+1) = \left( 1 - \frac{hA}{c_p\rho V}t_s \right) T_c(k) + \frac{hA}{c_p\rho V}t_s (u_1(k) - q_a(k)), \quad (17)$$

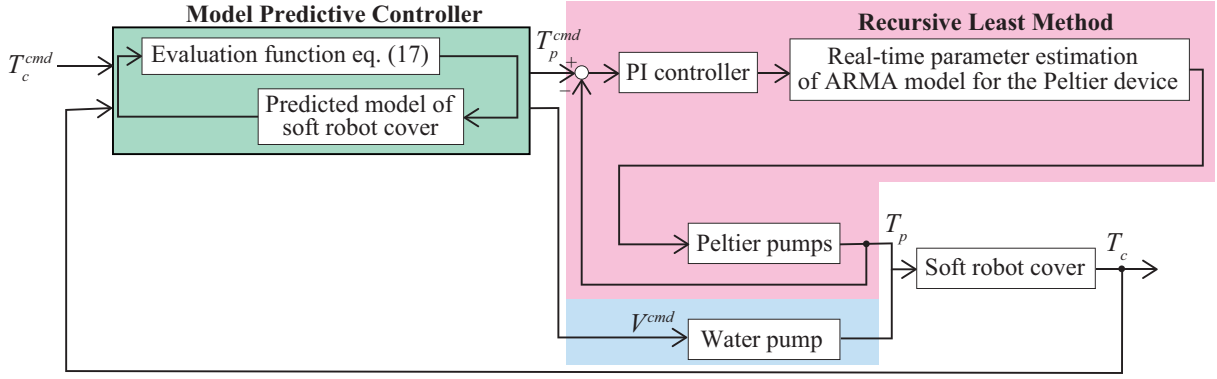


Fig. 7. Control system of the robot cover.

where  $k$  denotes the discrete time. The cost function with the constraints are calculated as

$$\min \left[ \sum_{i=1}^H \|\hat{T}_c(k+i|k) - T_c^{cmd}(k+i|k)\|_{W_1}^2 + \sum_{i=0}^{H-1} \|\hat{u}_1(k+i|k)\|_{W_2}^2 \right] \quad (18)$$

subject to

$$T_c(k+1) = \left(1 - \frac{hA}{c_p \rho V} t_s\right) T_c(k) + \frac{hA}{c_p \rho V} t_s u_1(k) \quad (19)$$

$$T_{\min}^{\text{th}} \leq u_1(k) \leq T_{\max}^{\text{th}}, \quad (20)$$

where  $H$ ,  $W_1$ ,  $W_2$ ,  $t_s$ ,  $T_{\min}^{\text{th}}$ , and  $T_{\max}^{\text{th}}$  stand for prediction horizon, weight values of the cost function, sampling time, and minimum and maximum value of threshold of the calculated input, respectively. The first term of (18) works for tracking the temperature of the cover  $T_c$  to its temperature command  $T_c^{cmd}$ , and the second one is for suppressing rapid change of the input  $u_1$ .

Figure 7 shows the whole control system of the robot cover. MPC generates the command for the Peltier pump derived from (18), using temperature response of the robot cover  $T_c$  and the constant voltage command for the water pump. Based on this command, the temperature of the Peltier pump is regulated by the proportional-integral (PI) controller. Some experimental results assessed the validity of the control system.

## V. EXPERIMENTS

### A. Outline

To assess the thermal display properties of the robot cover and its control system, temperature regulation experiments were conducted. The Fig. 8 shows the experimental setup. In the experiments, two TEMs 40mm × 40mm were used for heating and cooling the whole surface of the water tank 40mm × 80mm, of which both temperatures were controlled based on the command derived from the MPC. The heat sink and the fan was attached to the Peltier pumps for heat radiation at back sides. The thermocouples type  $T$  was attached to the robot cover. To adhere the Peltier pump to

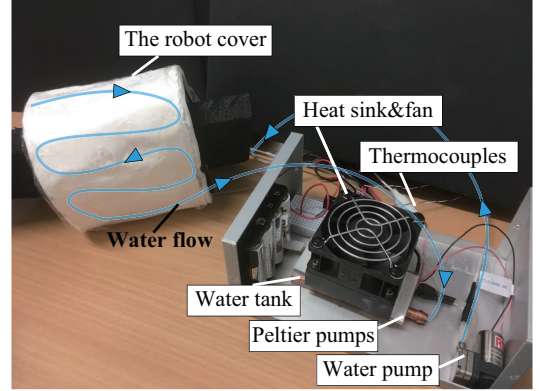


Fig. 8. The experimental setup.

TABLE IV  
PARAMETERS FOR EXPERIMENTS.

Parameter	Description	Value
$t_s$	sampling time	1.0 ms
$T_{\min}^{\text{th}}$	Minimum value of threshold of $T_p^{cmd}$	7 °C
$T_{\max}^{\text{th}}$	Maximum value of threshold of $T_p^{cmd}$	37 °C
$T_c^{cmd}$	Desired temperature command	21 °C–24 °C
$H$	Prediction horizon	100
$\lambda$	forget factor	0.995
$W_1$	Weight value of eq. (18)	0.6
$W_2$	Weight value of eq. (18)	0.05
$K_p$	Proportional gain	0.06
$K_i$	Integral gain	0.01

the water tank, the sheathed thermocouple type  $K$  that is a very thin temperature sensor we assembled at each control surface side of the Peltier pump. The temperature command  $T_c^{cmd}$  was set to 21–24°C, respectively. The parameters for the experiments were summarized in Table IV. As for the model parameters of the water system, the theoretical values and identification results shown in Table III in Sec. III-B.3 are used.

### B. Experimental results

Figures. 9 and 10 show the experimental results of temperature control to 23°C and 21°C, respectively. In both cases, the temperature command for the Peltier pump  $T_p^{cmd}$  is

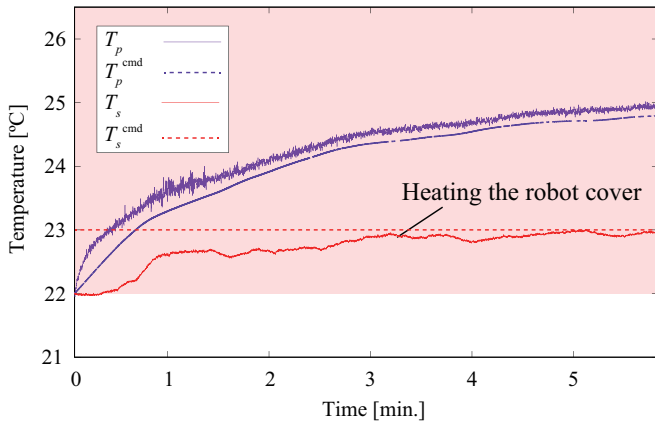


Fig. 9. Experimental results of heating the robot cover.

generated so that the temperature of the robot cover  $T_c$  meets its commanded  $T_c^{\text{cmd}}$ , and the response of the Peltier pump achieved the command. These experimental results show that the control system of the robot cover is functioning properly. Figure 11 shows the experimental results comparing various temperature commands. Here, the dotted line stands for each temperature command, and the responses approached its command, respectively. These experimental results show that the temperature of the robot cover can be controlled to the desired temperature within this temperature range.

There is still a problem in this prototype: the temperature response of the robot cover is slow (this is not critical when compared to human body thermal regulation system), and the controllable temperature range is limited (it has to be anyway, but we must target at least those acceptable by human touch). This is because the urethane pipe has low heat conductivity, and the gel layer is still relatively thick for conducting heat from the water. The thermal properties can be improved by replacing some materials of the robot cover because we have already tested some fundamental experiments for confirming it. Yet, the main contribution of this letter is the new design of the robot cover to investigate later the contribution of softness and thermal rendering for a secure and a pleasant feeling to a human touch. In future works, we aim at solve these problems based on the knowledge acquired from this prototype.

## VI. CONCLUSION AND FUTURE WORK

We designed a prototype of a new robot cover that gathers both softness and thermal display rendering capabilities. This cover is composed of two kinds of soft materials: one thin, a gel with high heat conductivity and relatively high mass density; the other, a soft foam with low heat conductivity and low mass density. Between the two we embedded soft pipes in which flow closed-circuit water that can be heated or cooled. We devised a system and a MPC controller that regulate the temperature for a given water flow. The parameters identification and models used are assessed together with validating this first prototype that already reveal several shortcomings improvements.

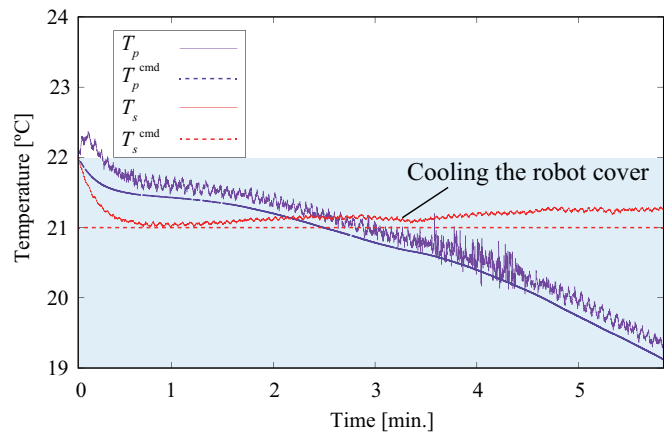


Fig. 10. Experimental results of cooling the robot cover.

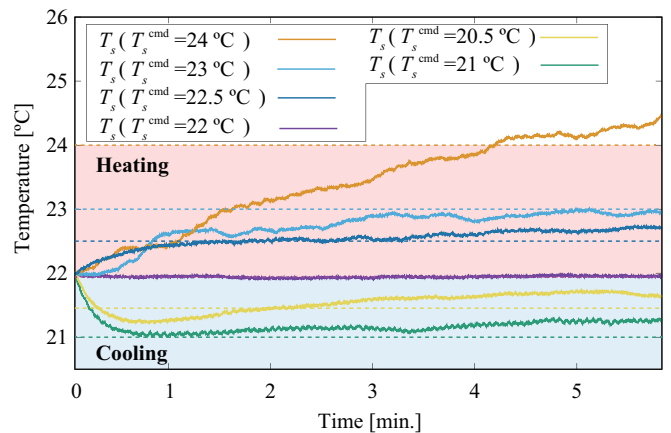


Fig. 11. Experimental results comparing to various commands.

For future work, we envision to ameliorate the materials we are using by pairing several variants customized and provided by Mitsui Chemicals Japan. We are discussing the possibility to built-in the pipes with the material manufacturing (i.e not using urethane pipes). We will improve the controller by considering water flow regulation as either a non-linear system controller or as an inter-switched linear system. We will also consider thermal observers to detect human touch. We shall as well coat on the surface fine different patterns in order to study pleasantness by varying softness, thermal rendering and surface texturing. On a long term, we believe that we might derive pipes to address motor cooling and cover thermal rendering in the same system. Indeed, we can consider that heating the water could be made from the actuator to dedicate the Peltier pumps (or another system) mainly for cooling purposes.

## ACKNOWLEDGMENT

The authors would like to thank Dr. Tatsuya Tokunaga, Mr. Masakazu Kageoka, and Mr. Kenji Iida from Mitsui Chemicals for providing the prototype of the soft robot cover.

## REFERENCES

- [1] H. Olausson, J. Cole, K. Rylander, F. McGlone, Y. Lamarre, B. G. Wallin, H. Krämer, J. Wessberg, M. Elam, M. C. Bushnell, and Å. Vallbo, "Functional role of unmyelinated tactile afferents in human hairy skin: sympathetic response and perceptual localization," *Experimental Brain Research*, vol. 184, no. 1, pp. 135–140, Jan 2008.
- [2] F. McGlone, J. Wessberg, and H. Olausson, "Discriminative and affective touch: Sensing and feeling," *Neuron*, vol. 82, no. 4, pp. 737–755, 2014.
- [3] M. Wiertelowski, C. Hudin, and V. Hayward, "On the 1/f noise and non-integer harmonic decay of the interaction of a finger sliding on flat and sinusoidal surfaces," in *IEEE World Haptics Conference*, June 2011, pp. 25–30.
- [4] A. Klöcker, M. Wiertelowski, V. Théate, V. Hayward, and J.-L. Thonnard, "Physical factors influencing pleasant touch during tactile exploration," *Plos ONE*, vol. 8, no. 11, pp. 1–8, 11 2013.
- [5] R. Ackerley, H. Backlund Wasling, J. Liljencrantz, H. Olausson, R. D. Johnson, and J. Wessberg, "Human c-tactile afferents are tuned to the temperature of a skin-stroking caress," *Journal of Neuroscience*, vol. 34, no. 8, pp. 2879–2883, 2014.
- [6] K. Salminen, V. Surakka, J. Raisamo, J. Lylykangas, R. Raisamo, K. Mäkelä, and T. Ahmaniemi, "Cold or hot? how thermal stimuli are related to human emotional system?" in *Haptic and Audio Interaction Design*, I. Oakley and S. Brewster, Eds. Berlin, Heidelberg: Springer Berlin Heidelberg, 2013, pp. 20–29.
- [7] J. Nie, M. Park, A. L. Marin, and S. S. Sundar, "Can you hold my hand? physical warmth in human-robot interaction," in *ACM/IEEE International Conference on Human-Robot Interaction*, March 2012, pp. 201–202.
- [8] E. Park and J. Lee, "I am a warm robot: the effects of temperature in physical human-robot interaction," *Robotica*, vol. 32, no. 1, pp. 133–142, 2014.
- [9] A. Alspach, J. Kim, and K. Yamane, "Design of a soft upper body robot for physical human-robot interaction," in *IEEE-RAS International Conference on Humanoid Robots*, Nov 2015, pp. 290–296.
- [10] B. Shih, D. Drotman, C. Christianson, Z. Huo, R. White, H. I. Christensen, and M. T. Tolley, "Custom soft robotic gripper sensor skins for haptic object visualization," in *IEEE/RSJ International Conference on Intelligent Robots and Systems*, Sep. 2017, pp. 494–501.
- [11] T. Kim, S. J. Yoon, and Y. Park, "Soft inflatable sensing modules for safe and interactive robots," *IEEE Robotics and Automation Letters*, vol. 3, no. 4, pp. 3216–3223, Oct 2018.
- [12] C. Larson, B. Peele, S. Li, S. Robinston, M. Totaro, L. Beccai, B. Mazzolai, and R. Shepherd, "Highly stretchable electroluminescent skin for optical signaling and tactile sensing," *Science*, vol. 351, no. 6277, pp. 1071–1074, 2016. [Online]. Available: <https://science.sciencemag.org/content/351/6277/1071>
- [13] T. P. Tomo, M. Regoli, A. Schmitz, L. Natale, H. Kristanto, S. Somlor, L. Jamone, G. Metta, and S. Sugano, "A new silicone structure for uskin—a soft, distributed, digital 3-axis skin sensor and its integration on the humanoid robot icub," *IEEE Robotics and Automation Letters*, vol. 3, no. 3, pp. 2584–2591, July 2018.
- [14] A. Cirillo, F. Ficuciello, C. Natale, S. Pirozzi, and L. Villani, "A conformable force/tactile skin for physical human-robot interaction," *IEEE Robotics and Automation Letters*, vol. 1, no. 1, pp. 41–48, Jan 2016.
- [15] J. C. Case, M. C. Yuen, J. Jacobs, and R. Kramer-Bottiglio, "Robotic skins that learn to control passive structures," *IEEE Robotics and Automation Letters*, vol. 4, no. 3, pp. 2485–2492, July 2019.
- [16] J. R. Guadarrama-Olvera, E. Dean-Leon, F. Bergner, and G. Cheng, "Pressure-driven body compliance using robot skin," *IEEE Robotics and Automation Letters*, vol. 4, no. 4, pp. 4418–4423, Oct 2019.
- [17] Y. Park, B. Chen, and R. J. Wood, "Design and fabrication of soft artificial skin using embedded microchannels and liquid conductors," *IEEE Sensors Journal*, vol. 12, no. 8, pp. 2711–2718, Aug 2012.
- [18] A. Gruebele, J. Roberge, A. Zerbe, W. Ruotolo, T. M. Huh, and M. R. Cutkosky, "A stretchable capacitive sensory skin for exploring cluttered environments," *IEEE Robotics and Automation Letters*, vol. 5, no. 2, pp. 1750–1757, April 2020.
- [19] G. Cannata, M. Maggiali, G. Metta, and G. Sandini, "An embedded artificial skin for humanoid robots," in *IEEE International Conference on Multisensor Fusion and Integration for Intelligent Systems*, Aug 2008, pp. 434–438.
- [20] S. Gallo, L. Santos-Carreras, G. Rognini, M. Hara, A. Yamamoto, and T. Higuchi, "Towards multimodal haptics for teleoperation: Design of a tactile thermal display," in *IEEE International Workshop on Advanced Motion Control*, March 2012, pp. 1–5.
- [21] A. Manasrah, N. Crane, R. Guldiken, and K. B. Reed, "Perceived cooling using asymmetrically-applied hot and cold stimuli," *IEEE Transactions on Haptics*, vol. 10, no. 1, pp. 75–83, Jan 2017.
- [22] G. J. Monkman and P. M. Taylor, "Thermal tactile sensing," *IEEE Transactions on Robotics and Automation*, vol. 9, no. 3, pp. 313–318, June 1993.
- [23] L. A. Jones and H. Ho, "Warm or cool, large or small? the challenge of thermal displays," *IEEE Transactions on Haptics*, vol. 1, no. 1, pp. 53–70, Jan 2008.
- [24] M. Guiatni, A. Benallegue, and A. Kheddar, "Learning-based thermal rendering in telepresence," in *Haptics: Perception, Devices and Scenarios*, M. Ferre, Ed. Berlin, Heidelberg: Springer Berlin Heidelberg, 2008, pp. 820–825.
- [25] H. Kajimoto and L. A. Jones, "Wearable tactile display based on thermal expansion of nichrome wire," *IEEE Transactions on Haptics*, vol. 12, no. 3, pp. 257–268, July 2019.
- [26] A. Drif, J. Citerin, and A. Kheddar, "Thermal bilateral coupling in teleoperators," in *IEEE/RSJ International Conference on Intelligent Robots and Systems*, Aug 2005, pp. 1301–1306.
- [27] M. Guiatni and A. Kheddar, "Modeling Identification and Control of Peltier Thermoelectric Modules for Telepresence," *Journal of Dynamic Systems, Measurement, and Control*, vol. 133, no. 3, 03 2011, 031010. [Online]. Available: <https://doi.org/10.1115/1.4003381>
- [28] Y. Osawa and S. Katsura, "Thermal propagation control using a thermal diffusion equation," *IEEE Transactions on Industrial Electronics*, vol. 65, no. 11, pp. 8809–8817, Nov 2018.
- [29] A. Bolotnikova, S. Courtois, and A. Kheddar, "Multi-contact planning on humans for physical assistance by humanoid," *IEEE Robotics and Automation Letters*, vol. 5, no. 1, pp. 135–142, 2020.
- [30] J. P. Holman, *Heat transfer*. McGraw-Hill, Inc, New York, 1990, vol. 1.
- [31] M. Battaglia, L. Blanchet, A. Kheddar, S. Kajita, and K. Yokoi, "Combining haptic sensing with safe physical interaction," in *IEEE/RSJ International Conference on Intelligent Robotics and Systems*, Saint Louis, MO, USA, 11–15 October 2009, pp. 231–236.
- [32] Y. G. GUREVICH and J. E. VELAZQUEZ-PEREZ, *Peltier Effect in Semiconductors*. American Cancer Society, 2014. [Online]. Available: <https://onlinelibrary.wiley.com/doi/abs/10.1002/047134608X.W8206>
- [33] M. Guiatni, A. Drif, and A. Kheddar, "Thermoelectric modules: Recursive non-linear arma modeling, identification and robust control," in *Annual Conference of the IEEE Industrial Electronics Society*, Nov 2007, pp. 568–573.
- [34] S. Adachi, *A Basic System Identification (Japanese)*. Tokyo Denki University Press, 2009.
- [35] H. Gräber, "Der wärmeübergang in glatten rohren, zwischen parallelen platten, längs der ebenen platte, in ringspalten und längs rohrbündeln bei exponentieller wärmeflussverteilung in erzwungener laminarer oder turbulenter strömung. eur 4381.= the heat transfer in smooth tubes, between parallel plates along the flat plate annular gaps and along tube bundles in exponential heat flux distribution in forced laminar or turbulent flow. eur 4381." *International Journal of Heat and Mass Transfer*, vol. 13, no. 11, pp. 1645–1703, 1970.